Multiple Encapsulated Electrode Plasma Actuator Effect on Aerofoil-Wake Interaction

Rasool Erfani* Amir Keshmiri†

School of Engineering, Manchester Metropolitan University, Manchester, M1 5GD, UK

School of MACE, The University of Manchester, Manchester, M13 9PL, UK

Tohid Erfani‡

Department of Civil Engineering, University College London, London, WC1E 6BT, UK

Konstantinos Kontis§

School of MACE, The University of Manchester, Manchester, M13 9PL, UK

Dielectric barrier discharge (DBD) plasma actuators have received considerable attention by many researchers for various flow control applications. Having no moving parts, being light-weight, easily manufacturable, and their ability to respond almost instantly are amongst the advantages which has made them a popular flow control device especially for application on aircraft wings. The new configuration of DBDs which uses multiple encapsulated electrodes (MEE) has been shown to produce a superior and more desirable performance over the standard actuator design. The objective of the current study is to examine the effect of this new actuator configuration on the aerodynamic performance of an aerofoil under wake interaction conditions. The plasma actuator is placed at the leading edge of a symmetric NACA 0015 aerofoil which corresponds to the location of the leading edge slat. The aerofoil is operated in a chord Reynolds number of 0.2×10^6. Surface pressure measurements along with the mean velocity profile of the wake using pitot measurements are used to determine the lift and drag coefficients, respectively. The results show an increase in the lift coefficient. It is also demonstrated that the drag coefficient decreases at all the measured angles of attacks.

I. Introduction

Flow control is the manipulation of flow characteristics to yield desirable effects. There are two categories of flow control devices: passive and active. Although passive methods which are always in a fixed state are relatively simpler to design and manufacture, they are only effective over a small range. Therefore, when dealing with unsteady motion, such as wake interaction with aerofoils, active flow control is the dominant choice. One of the disadvantageous of active flow control is the requirement of additional power.

The use of plasma as an active flow control medium has received considerable interest during the past decade.[1,2,3,4,5] While plasma was first identified as the fourth state of matter in 1879 and is well known to the physics community, it is a relative newcomer to the field of aerodynamics. The first recorded use of plasma for flow control was by Velkoff and Ketcham[6] who used a corona discharge to manipulate the transition point on a flat plate. The use of the 'ionic wind' generated by a corona discharge was the main focus of research attention until the late 1990's. In 1998 a new configuration of electrodes was presented by Roth et al.[7] that produced a One Atmosphere Uniform Glow Discharge Plasma (OAUGDP). This configuration was able to produce a jet in still air and manipulate the boundary layer of a flat plate.

Plasma actuators require no moving parts in converting electrical energy into kinetic energy, use a simple system structure, can operate over a broad frequency range and can be used instantaneously, making them

*Assistant Professor, AIAA Member, Email: *r.erfani@mmu.ac.uk*

†Assistant Professor, AIAA Member

‡Research Associate, AIAA Member

§Professor, School of MACE, AFAIAA

ideal for flow control purposes. The simple actuator design and ease of construction allows the actuator to be retro-fitted to existing aircraft and are also easy to manufacture and service. Previous studies have shown that dielectric barrier discharge (DBD) plasma actuators are efficient in different flow control applications: boundary layer manipulation,[8,9,10,11,12] lift augmentation on a wing section,[13] transition point manipulation,[14] and in particular in the field of separation control.[15,16,17,18,19]

Their benefits have not been fully utilised on a large scale since the applicability of plasma actuators is limited by the maximum induced velocity it can achieve. Extensive works have been conducted on flow control[20] and in particular on optimisation of the performance of DBD plasma actuators at the University of Manchester. Multiple encapsulated electrode (MEE)-DBD plasma actuator has shown its improved performance over the conventional DBD plasma actuator by increasing the induced jet velocity at a lower power consumption.[21,22,23]

In aeronautics, most open and closed turbo-machineries, and other engineering disciplines the flow over an aerofoil is influenced by a wake which for instance is originated from the preceding aerofoil. Such a wake can reduce the lift and increase loads on the downstream aerofoil which can create dangerous conditions for flying vehicles. This makes the study of the wake influence on aerodynamic characteristic of the aerofoil necessary. The disturbances in external flow initiate and force transition of boundary layers from laminar to turbulence. Extensive analytical, numerical and experimental studies have been conducted on boundary layer-wake interaction.[24,25,26]

The aerodynamic characteristics under the influence of the preceding wake have also been studied in relation to the laminar-turbulent transition of the boundary layer over an aerofoil. It is expected that the boundary layer over the aerofoil becomes turbulent through a transition process caused by the interaction between the wake and the boundary layer.[27,28,29,30,31] In addition, there are some investigations regarding the studies of aerodynamic forces of flying vehicle facing the wake of an aircraft.[32,33]

Kornilov et al.[34] discussed the interaction between an incompressible two-dimensional turbulent wake produced by a symmetrical aerofoil at incidence and a boundary layer formed on a similar aerofoil immediately downstream. A significant reduction in the level of turbulence was found in the boundary layer of the downstream aerofoil when it is located in the wake periphery. They identified that the outer region of this interaction can be described by simple correlations traditionally used for the wake behind a circular cylinder. Fujisawa et al.[27] discussed the influence of the circular cylinder wake on the aerodynamic performance of an aerofoil. Their results indicated that due to the interactions between the fluid forces and the cylinder wake the drag force decreases and the lift force increases at relatively large angles of attack typically beyond $\alpha = 12$ degrees. Their results show an improvement in aerodynamic performance of the aerofoil due to the influence of cylinder wake except for the lift coefficient at $\alpha = 9$ to 12 degrees.

The performance of a MEE-DBD plasma actuator in manipulating the aerodynamic coefficients of a NACA 0015 aerofoil with a chord Reynolds number of 0.2×10^6 has been demonstrated. The description of the optimum design of MEE-DBD which has been used in the current study has been presented by Erfani et al.[35]

II. Apparatus and Instrumentation

A. Wind tunnel

The experiments were conducted in one of the subsonic wind tunnels at the Aero-Physics Laboratory in the school of MACE at The University of Manchester. The facility is an open-return low subsonic 'blower' with a 0.455 m square cross section by 1.4 m long test section. The ceiling and side walls are made of optical grade perspex to allow optical access for photography and visualisation. Turbulence in the test section is reduced by the presence of honeycombs located upstream of the test section. The turbulent intensity in the test section over the range of velocities used in the experiment is approximately 0.24 %. The wind tunnel speed was monitored using a pitot-static tube placed upstream of the models mounted within the test section.

B. Aerofoil

The aerofoil used in the experiments was a NACA 0015 constructed from perspex with a chord length, c, of 0.24 m and span of 0.40 m. The characteristics of this aerofoil are well documented in the literature and it exhibits well-behaved leading edge separation at high angles of attack. For minimising the end effects, end plates are mounted on the sides of the aerofoil made from optical grade perspex to allow visual access for flow

visualisation and measurements. The end plates were 0.685×0.457×0.01 m (length×height×thickness). The leading and trailing ends of the end plates were machined to have a 5 mm radius. The maximum blockage of the aerofoil which occurs at the highest incidence was estimated to be 3.9%. Therefore, tunnel blockage effect on the aerodynamic coefficients considered minimal and no correction in the measuremnets taken were necessary.

C. Cylinder

At the working chord Reynolds number of 0.2×10^6, the frequency of the wake of the aerofoil at zero incidence is measured as 120 Hz and a Strouhal number, $St=fD/U_\infty$, of the cylinder estimated to be 0.2, where f is the frequency of the wake, D is the diameter of the cylinder and U_∞ is the free-stream velocity.[36,37,38] Therefore, a cylinder which can generate a frequency similar to that of the aerofoil should have a diameter of 0.02 m.[27]

The vortex shedding of the cylinder depends strongly on its diameter and the distance between the cylinder and the aerofoil. This critical distance is found by Luk et al.[39] to be equal to the length of the vortex formation region of the circular cylinder measured without the presence of aerofoil, and is 1.5 times of the diameter of the cylinder behind it. The cylinder is placed between two end plates at 0.2 m upstream of the aerofoil.

D. Plasma actuator

The typical plasma actuator is a linear asymmetric arrangement of two electrodes separated by a dielectric material. One electrode is exposed to the air, while the other is encapsulated in the dielectric. A schematic illustration of such an actuator is depicted in Figure 1 for a standard and MEE-DBD actuator. A high voltage alternating current (a.c.) input, with typical voltages of 2 kV_{p-p} to 60 kV_{p-p} (peak to peak voltage) and frequencies of 300 Hz to 1 MHz is supplied to the exposed electrode while the encapsulated electrode is earthed. Typically, the plasma actuator is long and thin and is placed spanwise on the aerodynamic surface.

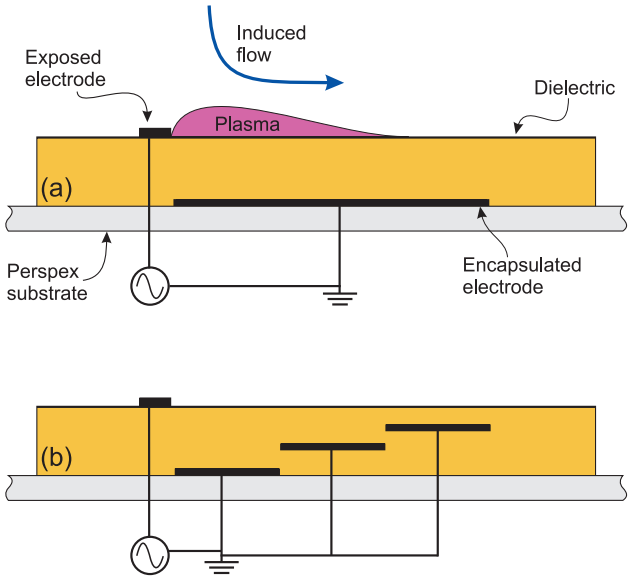

Figure 1. Typical configurations of standard DBD (a), and MEE-DBD plasma actuators (b)

The configuration of plasma actuator examined in the current investigation is shown in the schematic of Figure 3.[35] The actuator is placed at the leading edge while the interface of the exposed electrode and the first covered electrode is located at x/c = 0. The encapsulated electrodes are aligned so that there is no offset between the edges of successive electrodes. All the electrodes are tinned copper foils, 74 μm thick and 200 mm in length, in the spanwise direction. Layered Kapton tape was used as a dielectric material with each layer having a 60 μm thickness.

Dimensions and placement of the electrodes are also provided in Figure 3. The offset listed in figure is the distance measured from the downstream edge of the exposed electrode. To have a uniform plasma along

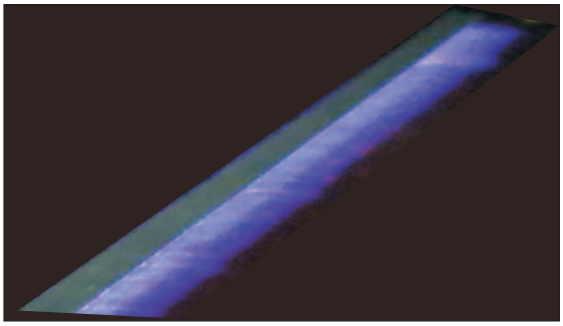

Figure 2. Photograph of plasma created on a DBD plasma actuator

the span, a small amount of overlap is applied between the downstream edge of the exposed electrode and upstream edge of the first encapsulated one.

	Width [mm]	Depth [mm]	Offset [mm]
Exposed electrode	5	0	0
A	5	0.24	0
B	40	0.48	5
C	5	0.18	45

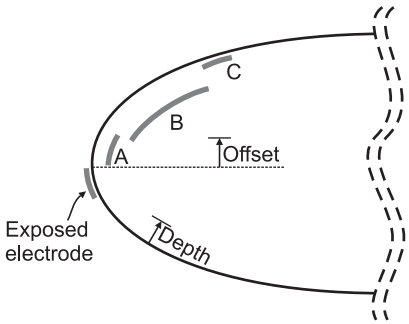

Figure 3. Aerofoil actuator configuration at the leading edge (figure not to scale)

The actuator was controlled by a LabView program where the wave shape, driving frequency, modulation frequency and corresponding duty cycles are controlled. This signal was provided via National Instruments PCI-6713 to a control circuit board that was also connected to a Volkraft 3610 power supply capable of outputting 360 W. The powered control signal is then connected to a transformer cascade which provides the high voltage signal to drive the actuator. The transformer is capable of a maximum 40 kV_{p-p} at driving frequencies up to 30 kHz.

The voltage supplied to the exposed electrode is measured using a LeCroy PPE-20 kV high voltage probe while the current is monitored using a current probe attached to the transformer cascade output. The two probes are connected to a Picoscope 3206, 250 MHz oscilloscope connected to a PC so the output signals can be monitored and recorded.

The actuator spanned most of the width of the leading edge of aerofoil. A narrow gap was left at the centre line due to the presence of pressure taps along chordwise direction. However, both sides were electrically connected. A recess equal to the thickness of the actuator had been cut from the aerofoil in order to produce a flush surface after mounting the actuator without changing the profile shape of the aerofoil.

E. Pressure measurements

A total of 23 surface pressure ports with an internal diameter of 1.5 mm were aligned in the flow direction at the half-span location of the aerofoil. The pressure tubes were passed through the side wall of the test section and connected to a scanning pressure valve that selectively connected each pressure port to a single pressure transducer.

A separate rake of pitot probes was mounted on a traversing mechanism and located downstream of the aerofoil at its spanwise centre line. Discrete points, with 2.54 mm distance between each probe, were sampled across the wake to determine the total pressure profile. The rake was placed one chord length downstream of the trailing edge in order to be far from any recirculation region that might exist in the separated flow.

For all pressure measurements, data was recorded for 4 seconds at a sampling rate of 10 kHz and averaged for both lift and drag measurements.

III. Results and Discussion

Figure 4 illustrates the comparison between mean velocity profiles 50 mm from the exposed electrode working in quiescent conditions of a standard DBD and optimised MEE-DBD actuator. The measurements were obtained from PIV experiments on actuators mounted on a flat surface. The actuators were operated at 15 kV_{p-p} with a driving frequency of 10 kHz using a sine wave input and 100% duty cycle. This driving frequency provides the actuator with a clean sinusoidal input signal not experienced at the other frequencies. The power consumption of the actuator was approximately 15 W. Identical settings are used on the aerofoil. As it is evident from the plot, the MEE-DBD actuator creates a faster induced jet with a greater jet thickness. This behaviour was also observed at different locations along the actuator.

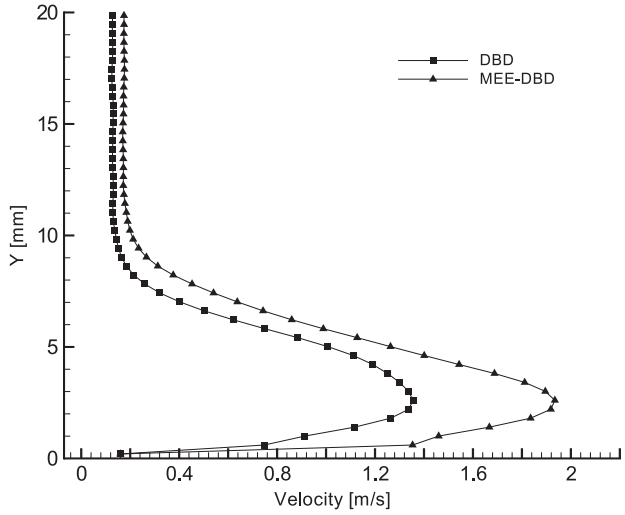

Figure 4. Mean velocity profiles obtained with 15 kV_{p-p} and 10 kHz at x = 50 mm

A. Aerofoil-wake interaction

The results in this section examine the effects of the leading edge MEE-DBD plasma actuator on the aerodynamic performance of the aerofoil at chord Reynolds number of 0.2×10^6, whilst in the wake of a circular cylinder.

The lift and drag coefficients of the aerofoil at various angles of attack facing the cylinder wake are presented in Figure 5(a) and Figure 5(b), respectively. The lift and drag coefficients of the plane aerofoil are also shown in the figure as the baseline case for comparative purposes. With the actuator in off mode, it is observed that up to the natural stall angle of the aerofoil $\alpha = 14^o$, the presence of the cylinder wake has an adverse effect on the performance of the aerofoil by reducing the lift and increasing the drag. However, at higher incidences the presence of the cylinder wake suppresses the stall and reduced the drag.

Figure 5 also includes the results for plasma on case. In all angles of attack, the actuator on case shows an increase in C_l compared to the actuator off case. Up to $\alpha = 14^o$ the drag coefficient does not change with increasing incidence for all cases, with the actuator on leading to a reduced level of drag compared to the actuator off case. After $\alpha = 14^o$ a significant rise in drag coefficient is observed for the baseline case whilst the presence of the cylinder wake suppresses the maximum drag coefficient. The drag coefficient begins to increase after 17^o for the cylinder wake case, but still does not approach the results without the cylinder case. This increase is believed to be due to the flow separation and formation of separation region at the trailing edge.

The pressure distribution on the aerofoil surface for a pre-stall angle of 11^o, and a post stall angle of 17^o is shown in Figures 6(a) and (b), respectively. At 11^o incidence the pressure distribution shows a reduction

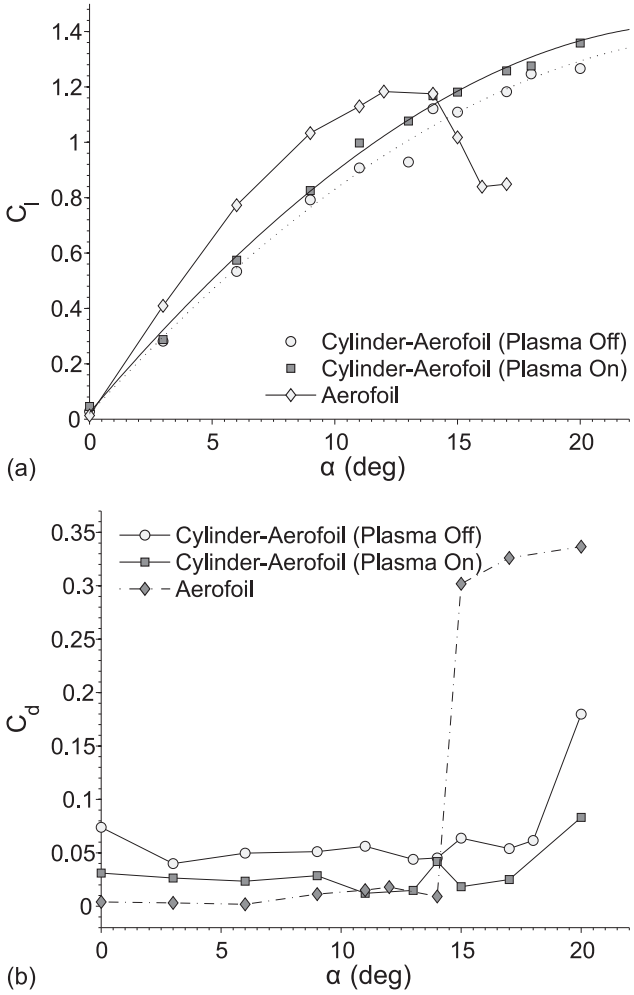

Figure 5. Lift coefficient (a), and drag coefficient (b)

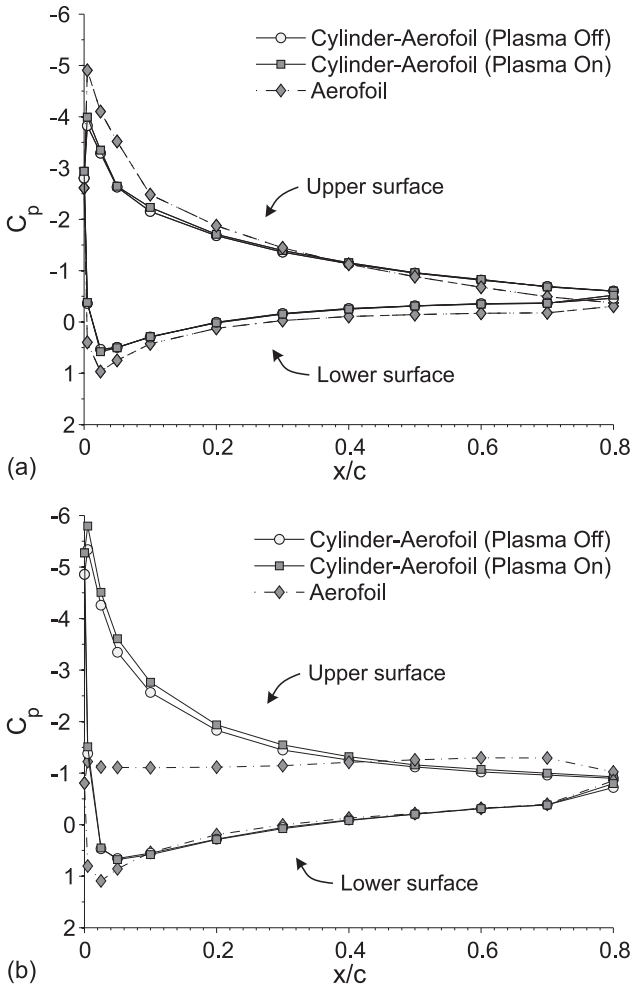

Figure 6. Pressure distribution on aerofoil surface for α = (a) 11^o (pre-stall), and (b) 17^o (post stall)

in pressure on the lower surface and increased pressure on the upper surface of the aerofoil compared to the baseline measurements of the aerofoil. No formation of a separated region was detected from the C_p curves in this range of pre-stall angles of attack. This justifies the constant values of C_d observed in Figure 5(b) for different angles. For the 17^o post stall case, the pressure distribution on the upper surface reveals a large decrease in pressure with the presence of the cylinder wake. This indicates an attached flow pattern on the surface due to the velocity fluctuations of the cylinder wake and its interaction with the boundary layer over the aerofoil. The separation of the boundary layer on the suction side is removed and a turbulent boundary layer forms over the surface. Flow over the lower surface of the aerofoil is also promoted to a turbulent state due to the influence of the cylinder wake which shows itself as a reduction in pressure values in Figure 6.

IV. Conclusions and future work

The influence of MEE-DBD plasma actuator proposed by Erfani et al.[35] on the aerodynamic performance of a NACA 0015 aerofoil has been investigated in aerofoil-wake interaction. Experiments were studied in a chord Reynolds number of 0.2×10^6. Overall, the new plasma actuator configuration produced an improvement in aerodynamic coefficients by increasing the lift and reducing the drag.

At high angles of attack, due to the wake excitation of the cylinder wake, the separation region at the suction side of the aerofoil was restrained, leading to the suppression of the stall angle. However, at all incidences the MEE actuator was able to increase the magnitude of the lift coefficient and decrease the level of drag coefficient.

Since a plasma actuator is designed to produce a steady two-dimensional wall jet in the flow direction on the upper surface, the pressure distribution on the lower surface remains unaffected. It would be an interesting study to examine the effect of the plasma actuators placed on the lower surface of the aerofoil.

Acknowledgments

The authors are indebted to the technical and administrative staff at Manchester Metropolitan University, the University of Manchester and University College London for their assistance. The authors would also like to thank the Institution of Mechanical Engineers (IMechE) for partially covering the costs of attending the conference.

References

[1]Enloe, C., McHarg, M., and McLaughlin, T., "Time-correlated force production measurements of the dielectric barrier discharge plasma aerodynamic actuator," *Journal of Applied Physics*, Vol. 103, 2008, pp. 073302.

[2]Enloe, C., McLaughlin, T., VanDyken, R., Kachner, K., Jumper, E., and Corke, T., "Mechanisms and responses of a single dielectric barrier plasma actuator: plasma morphology," *AIAA Journal*, Vol. 42, No. 3, 2004, pp. 589–594.

[3]Enloe, C., McLaughlin, T., VanDyken, R., Kachner, K., Jumper, E., Corke, T., Post, M., and Haddad, O., "Mechanisms and responses of a single dielectric barrier plasma actuator: geometric effects," *AIAA Journal*, Vol. 42, No. 3, 2004, pp. 595–604.

[4]Roth, J. and Dai, X., "Optimization of the aerodynamic plasma actuator as an electrohydrodynamic (EHD) electrical device," *44th AIAA Aerospace Sciences Meeting and Exhibit, Reno, Paper Number AIAA 2006-1203*, 2006, pp. 9–12.

[5]Roth, J.R. Sherman, D. and Wilkinson, S., "Electrohydrodynamic flow control with a glow-discharge surface plasma," *AIAA Journal*, Vol. 38, No. 7, 2000, pp. 1166–1172.

[6]Velkoff, H. and Ketcham, J., "Effect of an electrostatic field on boundary layer transition," *AIAA Journal*, Vol. 6, No. 7, 1968, pp. 1381–1383.

[7]Roth, J.R. Sherman, D. and Wilkinson, S., "Boundary layer flow control with a one atmosphere uniform glow discharge surface plasma," *36th Aerospace Sciences Meeting & Exhibit, Reno*, 1998.

[8]Porter, C., McLaughlin, T., Enloe, C., Font, G., Roney, J., and Baughn, J., "Boundary Layer Control Using a DBD Plasma Actuator," *45th AIAA Aerospace Sciences Meeting and Exhibit, Reno, Paper Number AIAA-2007-786*, 2007.

[9]Opaits, D., Roupassov, D., Starikovskaia, S., Starikovskii, A., Zavialov, I., and Saddoughi, S., "Plasma control of boundary layer using low-temperature non-equilibrium plasma of gas discharge," *AIAA Journal*, Vol. 1180, No. 43, 2005, pp. 10–13.

[10]Boxx, I., Rivir, R., Newcamp, J., and Woods, N., "Reattachment of a Separated Boundary Layer on a Flat Plate in a Highly Adverse Pressure Gradient Using a Plasma Actuator," *3rd AIAA Flow Control Conference, San Francisco, Paper Number AIAA 2006-3023*, 2006.

[11]Jacob, J., Rivir, R., Carter, C., and Estevadeordal, J., "Boundary layer flow control using AC discharge plasma actuators," *AIAA 2nd Flow Control Meeting, Paper Number AIAA-2004-2128*, 2004.

[12]Font, G., "Boundary layer control with atmospheric plasma discharges," *AIAA Journal*, Vol. 44, No. 7, 2006, pp. 1572–1578.

[13]Corke, T., Cavalieri, D., and Matlis, E., "Boundary-layer instability on sharp cone at Mach 3.5 with controlled input," *AIAA Journal*, Vol. 40, 2002, pp. 1015–1018.

[14]Grundmann, S. and Tropea, C., "Delay of Boundary-Layer Transition Using Plasma Actuators," *46th AIAA Aerospace Sciences Meeting and Exhibit, Paper Number AIAA-2008-1369*, 2008.

[15]He, C., Corke, T., and Patel, M., "Plasma flaps and slats: an application of weakly ionized plasma actuators," *Journal of Aircraft*, Vol. 46, No. 3, 2009, pp. 864–873.

[16]Post, M. and Corke, T., "Separation control using plasma actuators: dynamic stall vortex control on oscillating airfoil," *AIAA Journal*, Vol. 44, No. 12, 2006, pp. 3125–3135.

[17]Post, M. and Corke, T., "Separation control on high angle of attack airfoil using plasma actuators," *AIAA Journal*, Vol. 42, No. 11, 2004, pp. 2177–2184.

[18]Huang, J., Corke, T., and Thomas, F., "Plasma actuators for separation control of low-pressure turbine blades," *AIAA Journal*, Vol. 44, No. 1, 2006, pp. 51–57.

[19]Rethmel, C., Little, J., Takashima, K., Sinha, A., Adamovich, I., and Samimy, M., "Flow separation control over an airfoil with nanosecond pulse driven DBD plasma actuators," *49th AIAA Aerospace Sciences Meeting including the New Horizons Forum and Aerospace Exposition, Orlando, Florida, Paper Number AIAA-2011-487*, 2011.

[20]Hale, C., Amir, M., Kontis, K., Shah, N., and Wong, C., "Active and Passive Flow Control Studies at Subsonic Speeds at The University of Manchester," *46th AIAA Aerospace Sciences Meeting and Exhibit, Reno, Nevada, Paper Number AIAA-2008-283*, 2008.

[21]Hale, C., Erfani, R., and Kontis, K., "Plasma Actuators with Multiple Encapsulated Electrodes to Influence the Induced Velocity," *48th AIAA Aerospace Sciences Meeting Including the New Horizons Forum and Aerospace Exposition, Paper Number AIAA-2010-1223*, 2010.

[22]Hale, C., Erfani, R., and Kontis, K., "Plasma Actuators with Multiple Encapsulated Electrodes to Influence the Induced Velocity : Further Configurations," *40th Fluid Dynamics Conference and Exhibit, Paper Number AIAA-2010-5106*, No. 2010-5106, 2010.

[23]Erfani, R., Hale, C., and Kontis, K., "The Influence of Electrode Configuration and Dielectric Temperature on Plasma Actuator Performance," *49th AIAA Aerospace Sciences Meeting including the New Horizons Forum and Aerospace Exposition, Orlando, Paper Number AIAA-2011-955*, 2011.

[24]Squire, L., "Interactions between wakes and boundary-layers," *Progress in Aerospace Sciences*, Vol. 26, No. 3, 1989, pp. 261–288.

[25]Doligalski, T. and Walker, J., "The boundary layer induced by a convected two-dimensional vortex," *Journal of Fluid Mechanics*, Vol. 139, No. -1, 1984, pp. 1–28.

[26]Gartshore, I., Durbin, P., and Hunt, J., "The production of turbulent stress in a shear flow by irrotational fluctuations," *Journal of Fluid Mechanics*, Vol. 137, No. -1, 1983, pp. 307–329.

[27]Takagi, Y., Fujisawa, N., Nakano, T., and Nashimoto, A., "Cylinder wake influence on the tonal noise and aerodynamic characteristics of a NACA0018 airfoil," *Journal of Sound and Vibration*, Vol. 297, No. 3-5, 2006, pp. 563–577.

[28]Pfeil, H., Herbst, R., and Schroder, T., "Investigation of the laminar-turbulent transition of boundary layers disturbed by wakes," *American Society of Mechanical Engineers, International Gas Turbine Conference and Exhibit, 27 th, London, England*, 1982.

[29]Liu, X. and Rodi, W., "Experiments on transitional boundary layers with wake-induced unsteadiness," *Journal of Fluid Mechanics Digital Archive*, Vol. 231, 2006, pp. 229–256.

[30]Kyriakides, N., Kastrinakis, E., Nychas, S., and Goulas, A., "Aspects of flow structure during a cylinder wake-induced laminar/turbulent transition," *AIAA Journal*, Vol. 37, No. 10, 1999, pp. 1197–1205.

[31]Mailach, R. and Vogeler, K., "Wake-induced boundary layer transition in a low-speed axial compressor," *Flow, Turbulence and Combustion*, Vol. 69, No. 3, 2002, pp. 271–294.

[32]Bloy, A., West, M., and Lea, K., "Lateral aerodynamics interference between tanker and receiver in air-to-air refueling," *Journal of Aircraft*, Vol. 30, No. 5, 1993, pp. 705–710.

[33]Iversen, J. and Bernstein, S., "Trailing vortex effects on following aircraft," *Journal of Aircraft*, Vol. 11, 1974, pp. 60.

[34]Kornilov, V., PAILHAS, G., and AUPOIX, B., "Airfoil-boundary layer subjected to a two-dimensional asymmetrical turbulent wake," *AIAA Journal*, Vol. 40, No. 8, 2002, pp. 1549–1558.

[35]Erfani, R., Erfani, T., Utyuzhnikov, S., and Kontis, K., "Optimisation of Multiple Encapsulated Electrode Plasma Actuator," *Aerospace Science and Technology*, 2012.

[36]Zdravkovich, M., *Flow Around Circular Cylinders: Fundamentals*, Oxford science publications, Oxford University Press, 1997.

[37]Nakagawa, T., "A formation mechanism of alternating vortices behind a circular cylinder at high Reynolds number," *Journal of Wind Engineering and Industrial Aerodynamics*, Vol. 25, No. 1, 1986, pp. 113–129.

[38]Roshko, A., "Experiments on the flow past a circular cylinder at very high Reynolds number," *Journal of Fluid Mechanics*, Vol. 10, No. 03, 1961, pp. 345–356.

[39]Luk, K., So, R., Kot, S., Lau, Y., and Leung, R., "Airfoil Vibration Due to Upstream Alternating Vortices Generated by a Circular Cylinder," *ASME Applied Mechanics Division-Publication-AMD*, Vol. 253, No. A, 2002, pp. 79–88.